



HAL
open science

Fundamental mode selection thanks to metamaterial wall insertion in waveguides

Lucille Kuhler, Nathalie Raveu, Gwenn Le Fur, Luc Duchesne

► **To cite this version:**

Lucille Kuhler, Nathalie Raveu, Gwenn Le Fur, Luc Duchesne. Fundamental mode selection thanks to metamaterial wall insertion in waveguides. *Engineering Reports*, 2021, 10.1002/eng2.12363 . hal-03108181

HAL Id: hal-03108181

<https://enac.hal.science/hal-03108181>

Submitted on 13 Jan 2021

HAL is a multi-disciplinary open access archive for the deposit and dissemination of scientific research documents, whether they are published or not. The documents may come from teaching and research institutions in France or abroad, or from public or private research centers.

L'archive ouverte pluridisciplinaire **HAL**, est destinée au dépôt et à la diffusion de documents scientifiques de niveau recherche, publiés ou non, émanant des établissements d'enseignement et de recherche français ou étrangers, des laboratoires publics ou privés.

Fundamental Mode Selection Thanks to Metamaterial Wall Insertion in Waveguides

Lucille Kuhler, Nathalie Raveu, Gwenn Le Fur, and Luc Duchesne

Abstract—In this paper, a new application of metamaterials is put forward, the selection of the fundamental mode of waveguides. To demonstrate this new application, the Modal Expansion Theory (MET) hybridized with a 2D Finite-Element-Method (FEM) is used. The procedure to design metamaterial waveguides using the MET is also introduced. This method is used to design a corrugated waveguide with a TM_{01} mode as fundamental mode, knowing that in metallic waveguide the fundamental mode is the TE_{11} . As a proof of concept, this metamaterial waveguide is fabricated as well as the metallic waveguide. Both waveguides are excited with the TE_{11} mode, which results in a standard propagation of this mode in the metallic waveguide, and no propagation in the corrugated waveguide. To excite the TM_{01} , a new Coaxial to Waveguide Transition (CWT) is developed and presented in the paper. Both, simulations and experiments are carried out in order to verify and prove the fact that the fundamental mode of the corrugated waveguide is the TM_{01} mode.

Index Terms—Coaxial to waveguide transition, cylindrical waveguide, fundamental mode, metamaterials, modal expansion theory (MET).

I. INTRODUCTION

METAMATERIALS are well known and widely used in the industry [1]–[4]. Thanks to their space arrangement, they can be designed to exhibit special electromagnetic properties, usually not encountered in natural materials [5], such as a relative permittivity and/or a permeability smaller than 1 or less than 0 [6]–[8]. In most applications, metamaterials are used to reduce the waveguide size, and therefore its weight [9]–[14] or to control the field at the horn antenna aperture [3], [14]–[17]. In the past few years, a new method of characterization of waveguides with anisotropic walls and metamaterial walls has been put forward: the Modal

Expansion Theory (MET) [14], [18]–[23]. In [19], only waveguides with fixed anisotropic walls were studied. By combining the main algorithm of the MET and a 2-D Finite Element Method (FEM) code, the study of waveguides with 2-D metamaterials is realized [20]–[23]. In these articles, metamaterials are replaced by their equivalent surface impedances at any given volume height. These impedances are dependent on the frequency, the incidence angle and on the propagating mode. Thus, the MET returns the propagation characteristics of 2-D metamaterial waveguides. Moreover, the characterization is obtained drastically faster than when obtained using commercial software such as HFSS [21]–[23]. As a matter of fact, the 3-D problem is solved and reduced into a 2-D problem [20]–[23].

In this article, a new application of metamaterials in waveguides is proposed selecting the fundamental mode. In cylindrical metallic waveguides, the TE_{11} mode is the fundamental mode while the TM_{01} is the second propagating mode. However, the TM_{01} mode presents a circular symmetric pattern very useful for signals detection when coming from unknown directions [24]. In the space industry, the TM_{01} mode is particularly relevant for communications and satellites positioning [25], [26]. Another application domain of the TM_{01} mode is in High-Power Microwaves (HPMs) [27], [28]. Hence, the mode of interest in this article is the TM_{01} mode, and it is selected as the fundamental mode of the metamaterial waveguide. A new procedure to design the metamaterial based on the MET is also proposed in this article. First of all, the MET is applied to anisotropic waveguides [19] to find the impedances range allowing a TM_{01} fundamental mode. Then, the 2-D FEM code is used to design the metamaterial. As a matter of fact, the 2-D FEM code returns the equivalent surface impedances of the metamaterial. By calculating these impedances for different frequencies and incidence angles, the dimensions of the metamaterial can be found. Then the algorithm of the MET including the 2-D FEM code [21]–[23] is used to plot the dispersion diagram to verify that the TM_{01} is the fundamental mode.

In cylindrical waveguides, 2-D metamaterials are those with a θ invariance. There are plenty of 2-D metamaterials, some of which have already been presented in [21]–[23]. As a trade-off between the metamaterial design and the complexity of its fabrication, a corrugation is proposed in this work. While many articles deal with corrugated waveguide [29]–[35], the novelty of this method lies in the fact that all 2-D metamaterials can be studied. In case no corrugation achieves

Manuscript submitted July 20, 2020. This work was funded by the CNES and made in collaboration between the CNES, MVG Industries and the LAPLACE laboratory.

L. Kuhler was with the University of Toulouse, INPT, UPS, LAPLACE, ENSEEIHT, Toulouse 31071, France, in collaboration with the Centre National d'Etudes Spatiales (CNES), Toulouse 31400, France and also with MVG Industries, Villejust 91140, France. Now she is with the ENAC (French Civil Aviation University), TELECOM-EMA, Toulouse, 31055, France (e-mail: lucille.kuhler@enac.fr).

N. Raveu is with the University of Toulouse, INPT, UPS, LAPLACE, ENSEEIHT, Toulouse 31071, France (e-mail: raveu@laplace.univ-tlse.fr).

G. Le Fur is with the Centre National d'Etudes Spatiales (CNES), Toulouse 31400, France (e-mail: gwenn.lefur@cnes.fr).

L. Duchesne is with MVG Industries, Villejust 91140, France (e-mail: luc.duchesne@mvg-world.com).

the impedances range criteria, any 2-D metamaterial can be considered.

In this article, the main objective is to design a corrugated waveguide with a TM_{01} fundamental mode by using a new procedure based on the MET. Section II addresses the design of a waveguide with TM_{01} fundamental mode. A comparison with the equivalent classical waveguide is also performed. As a proof of concept this new waveguide is fabricated. In the third section, simulations and measurements are compared. Firstly, the new waveguide is tested with a TE_{11} excitation to prove that this mode is not a propagating mode. Then the TM_{01} is injected in this waveguide, and the propagation is confirmed. A new Coaxial to Waveguide Transition (CWT) is proposed to generate this particular mode.

II. WAVEGUIDE DESIGN WITH TM_{01} FUNDAMENTAL MODE

In classical cylindrical waveguides, the fundamental mode is the TE_{11} and the second one is the TM_{01} . However, it is possible to change the fundamental mode by adding an anisotropic wall [36]. In this article, a metamaterial with a θ invariance is proposed to achieve this goal. In part II.A, the design methodology to find the impedances range allowing a TM_{01} fundamental mode is given by using the MET for waveguides with fixed anisotropic wall [19]. In part II.B, the dimensions of the corrugation that respects this range are presented as well as the dispersion diagram of the corrugated waveguide obtained with the MET and the 2-D FEM code [21]–[23].

The cylindrical waveguide with metamaterial wall is considered invariant along the z -axis, the propagation axis. Therefore the electromagnetic field has an $e^{-jk_z z}$ dependence, with k_z the propagation constant along the z -axis.

A. Design Methodology

As explained in the introduction, the goal is to have a TM_{01} fundamental mode. Consequently, the external radius of the metamaterial waveguide is fixed by the metallic waveguide used as the reference. This metallic waveguide has an A section of 34.2 mm. Thus, the two first mode cutoff frequencies are imposed by the A radius and computed with (1) [37]:

$$\begin{cases} f_{cTE_{11}} = \frac{\chi'_{11}c}{2A\pi} = 2.57 \text{ GHz} \\ f_{cTM_{01}} = \frac{\chi_{01}c}{2A\pi} = 3.36 \text{ GHz}, \end{cases} \quad (1)$$

where χ'_{11} is the first zero of J'_1 derivative of Bessel first order function, χ_{01} the first zero of J_0 zero order Bessel function and c the free space light speed.

The MET [19] is, first, applied to cylindrical waveguides with fixed isotropic and anisotropic wall, as represented in Fig. 1. These waveguides have the same a radius smaller than A . As a matter of fact, A is fixed at 34.2 mm, and the a radius is the radius where the equivalent surface impedances of the metamaterial are computed. Therefore, the metamaterial is between A and a . For this application, a is equal to $4A/10$ in

order to have enough degree of freedom to design the metamaterial.

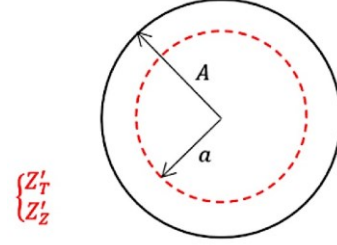


Fig. 1. Cylindrical waveguide with fixed isotropic anisotropic wall at the a radius.

The dispersion properties of the a waveguide vary by changing the surface impedances (Z'_T, Z'_Z). The dispersion diagrams of the different waveguides (with different combinations of surface impedances) are obtained with the MET [19] also allowing the identification of the propagating modes. Dispersion diagrams are represented in Fig. 2, which show the impedances range that permits the TM_{01} mode to propagate as fundamental mode with a cutoff frequency in the vicinity of 3 GHz. This choice of frequency is made in order to keep the same order of magnitude of the cutoff frequency of the TM_{01} mode in the metallic waveguide. This range is defined by (2):

$$\begin{cases} Z'_T \neq \frac{jZ_0}{2} \\ jZ_0 < Z'_Z \leq 2jZ_0. \end{cases} \quad (2)$$

Hence, the dimensions of the metamaterial are found in order to respect the impedances range (2).

B. Metamaterial Waveguide Design

1) Waveguide Wall Choice

Among different 2-D metamaterials, the corrugation is chosen because its fabrication is less complex. Corrugation in a waveguide induces metamaterial properties because it is a periodical structure and its depth is small compared to the wavelength. A unit cell of a corrugation is presented in Fig. 3. The dimensions that can be modified to comply with (2) are the d depth, the p periodicity and the w width. These dimensions are adjusted in order to have the (Z'_T, Z'_Z) equivalent surface impedances computed in the a radius in the range (2). These impedances are computed thanks to the 2-D FEM code. Finally, the resulting corrugation is represented in Fig. 3.

Fig. 4 confirms that the corrugation of Fig. 3 respects (2). Indeed, Z'_Z surface impedance varies between jZ_0 and $2jZ_0$ without reaching these values. Moreover, only the TM_{01} mode is propagating, consequently Z'_T is not equal to $jZ_0/2$.

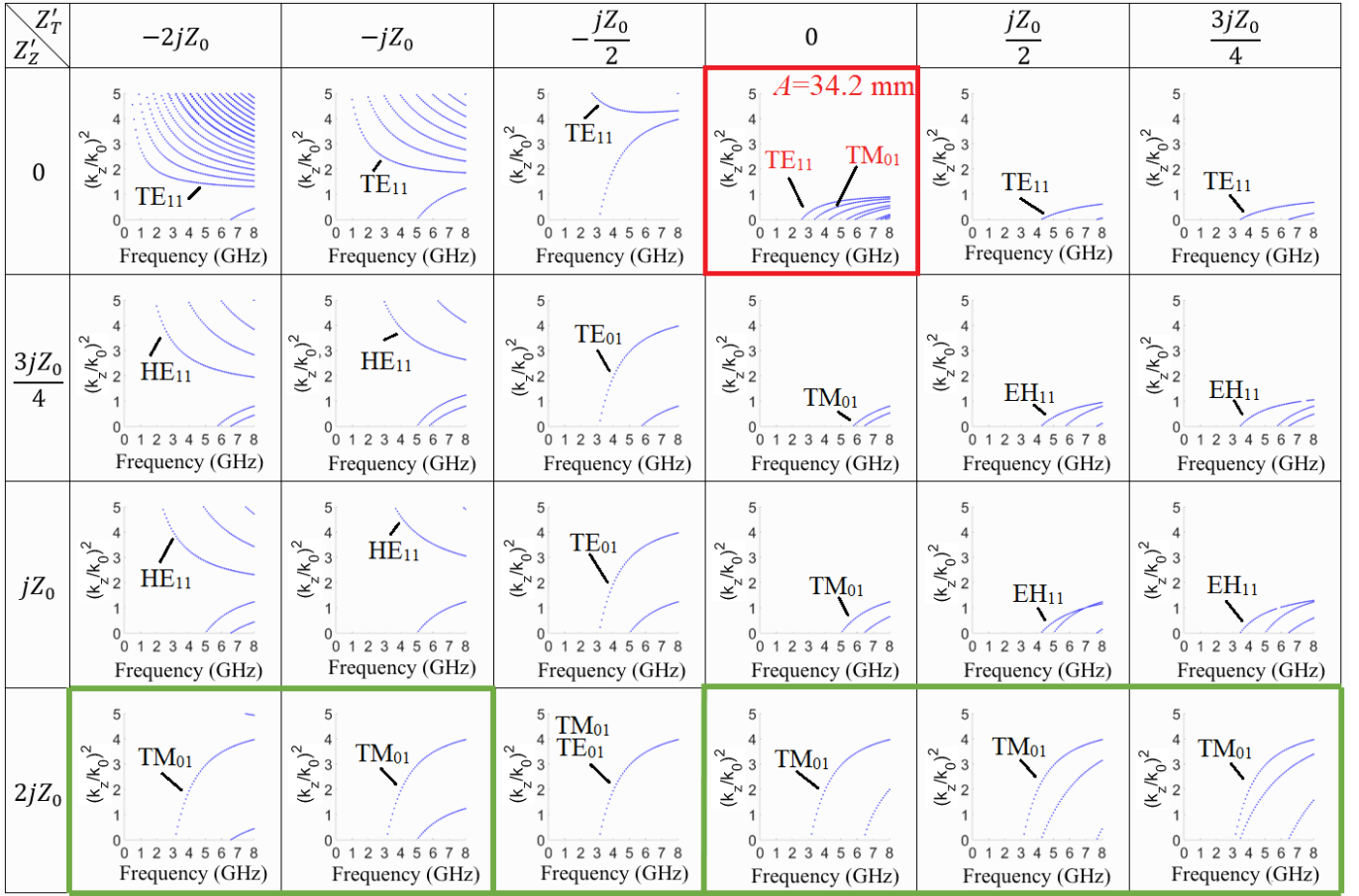


Fig. 2. An extract of the table with different values of the surface impedances fixed on the a radius. In red, the dispersion diagram of the metallic waveguide. In bold green line, the dispersion diagrams that have the TM_{01} fundamental mode with a cutoff frequency around 3 GHz.

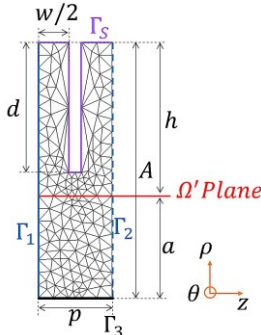


Fig. 3. Unit cell mesh and dimensions: $A = 34.2$ mm, $a = 13.68$ mm, $h = 20.52$ mm, $p = 11.5$ mm, $w = 8.5$ mm and $d = 17.4$ mm. On the Γ_s boundary a PEC condition is applied.

2) Dispersion Diagrams

To affirm that only the TM_{01} mode is propagating and that it is the fundamental mode, the dispersion diagram of the corrugated waveguide is plotted using the MET and the 2-D FEM code. However, as explained in [21]–[23], with this algorithm only $m = 0$ mode are obtained. Consequently, the commercial software is also used to plot the entire dispersion diagrams. To counter this issue, the MET is currently extended to deal with all metamaterials and all order modes with to 3-D FEM code.

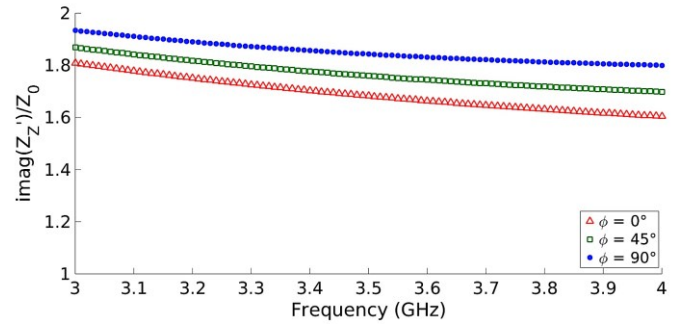


Fig. 4. The Z'_z surface impedance of the corrugation represented in Fig. 3.

Fig. 5 represents the dispersion diagrams of the metallic waveguide (triangles) and the corrugated one (dots for the MET and circles for HFSS).

The first mode of the corrugated waveguide is the TM_{01} mode and its cutoff frequency is 3.57 GHz. The second mode is the EH_{11} hybrid mode, its pattern is represented on the Fig. 6 [16], [17], [31], and its cutoff frequency is 4.7 GHz. According to Fig. 5, the TE_{11} mode is canceled and a new mode, the EH_{11} hybrid mode, appears at higher frequencies.

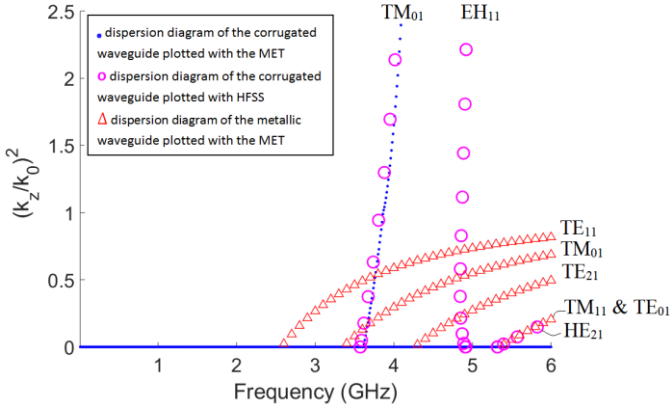


Fig. 5. Dispersion diagrams of the corrugated waveguide obtained with MET (dots) and HFSS (circles) and comparison with the metallic waveguide (triangles).

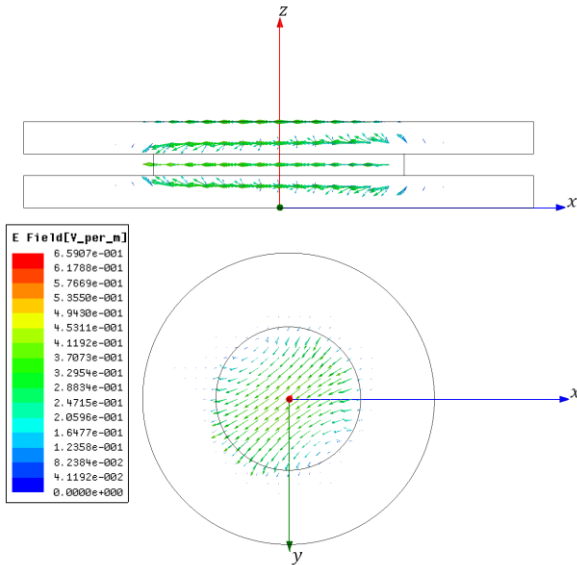


Fig. 6. The electric field of the EH_{11} mode in a section of the corrugated waveguide.

III. NUMERICAL AND EXPERIMENTAL RESULTS

To verify the metamaterial waveguide performances, it is necessary to measure the S-parameters of both waveguides (metallic and metamaterial) with two different excitations (TE_{11} and TM_{01}). Firstly, the TE_{11} mode is generated in the metallic waveguide to verify its propagation, then it is generated in the metamaterial waveguide where it is not expected to propagate. Secondly the TM_{01} mode is excited in both waveguides with a new Coaxial to Waveguide Transition (CWT). This mode should propagate into the corrugated waveguide. In the next parts, the excitation of the TE_{11} mode is explained and CWT for the TM_{01} is proposed. The corrugated waveguide, the metallic waveguide, the transitions and the CWT have been fabricated with a milling machine, as represented in Fig. 7a) and b).

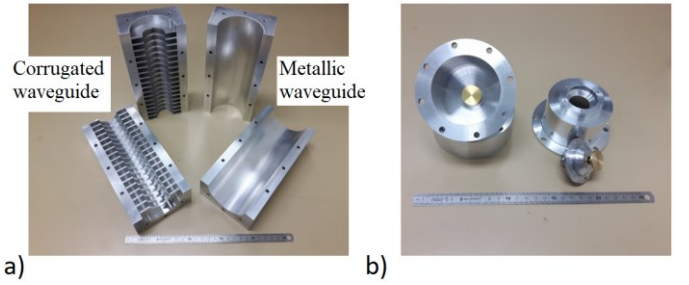


Fig. 7. a) The corrugated or metallic waveguides and b) the cylindrical CWT for TM_{01} generation.

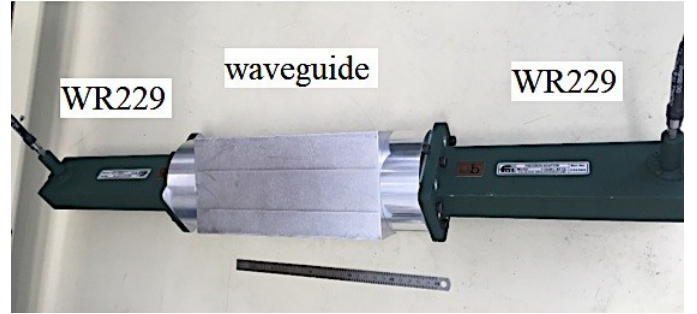


Fig. 8. Measurement setup for TE_{11} generation.

A. TE_{11} Excitation

To generate the TE_{11} fundamental mode of the metallic cylindrical waveguides, the WR229 calibration kit of the rectangular waveguide is used. To connect cylindrical and rectangular waveguides a transition is fabricated. This transition is not perfectly matched since the matching would be different for the metallic and the metamaterial waveguides. However, the goal of this experiment is to prove that the TE_{11} is not propagating in the corrugated waveguide and still propagating in the metallic waveguide. Fig. 8 represents the measurement setup to prove that the TE_{11} mode is not propagating.

The S-parameters are plotted in Fig. 9. The measured S-parameters of the corrugated waveguide, Fig. 9a) are compared to the S-parameters of the metallic waveguide, Fig. 9b). Fig. 9a) evidently confirms that no mode is propagating with the TE_{11} excitation in the corrugated waveguide within the [3, 4.7] GHz band, while in the metallic at least one mode is propagating, Fig. 9b) with a matching that is not perfect as explained at the beginning of this section.

B. TM_{01} Excitation

[27], [28], [38]–[43] deal with TM_{01} mode generation. However, the proposed designs are quite complicated. Looking at the TM_{01} mode field cartography, Fig. 10, a centered electric probe along the z-axis seems to be the easiest choice. A washer is placed at the feeding access end to improve the transmission bandwidth, shown in Fig. 11.

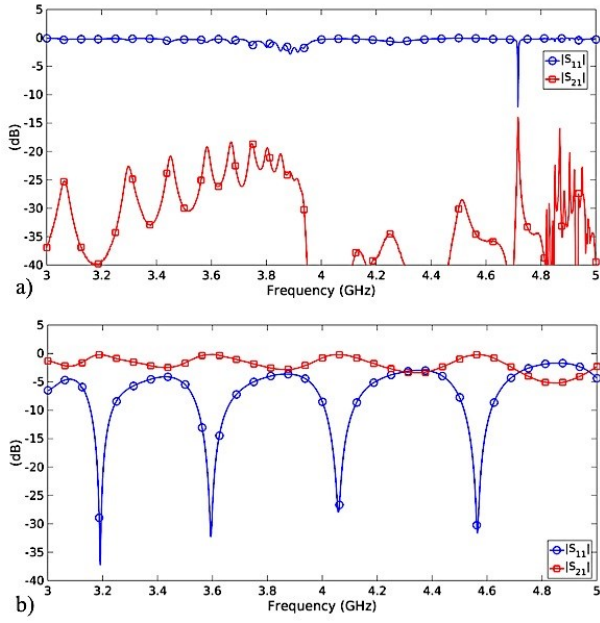


Fig. 9. a) The measured S-parameters of the corrugated waveguide and b) the measured S-parameters of the metallic waveguide with the TE_{11} feed. S_{11} is in blue circles while S_{21} is in red squares.

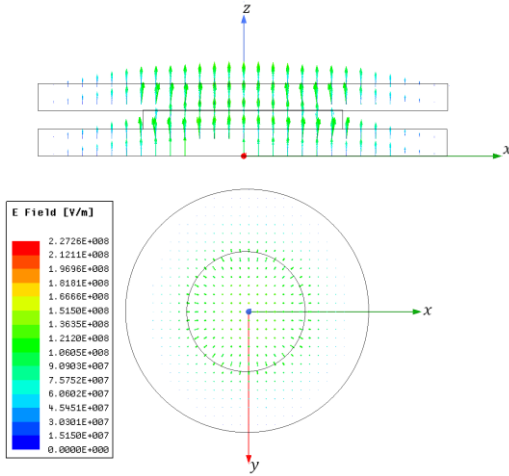


Fig. 10. The electric field of the TM_{01} mode in a section of the corrugated waveguide.

1) Measurement and Simulation Principles

Different simulations are realized in order to fully study the behavior of the proposed CWT before its manufacturing. These simulations are similar to calibrations made before measurements. A first simulation is performed to find the CWT S-parameters by connecting them directly, see Fig. 12. In HFSS, the waveports are deemed to remove the coaxial cable lengths.

The HFSS simulation returns the S-parameters of the structure in Fig. 12. Using a Matlab code, S-parameters are transformed into ABCD-parameters [44]. Then, ABCD-parameters of one CWT are isolated thanks to (3). In fact, both CWT are assumed to be identical.

$$[T_{CWT}] = [T_{struc}]^{1/2}, \quad (3)$$

where $[T_{CWT}]$ is the chain matrix of one transition, and $[T_{struc}]$ is the chain matrix of the structure in Fig. 12.

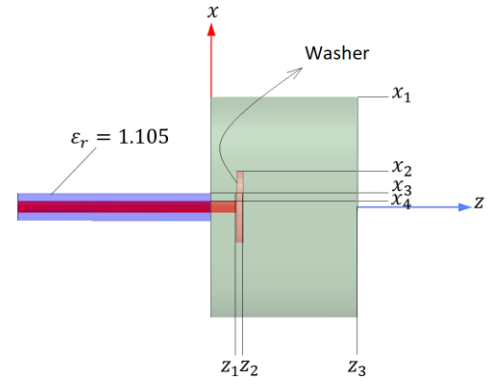


Fig. 11. The dimensions of the CWT: $z_1 = 8$ mm, $z_2 = 10$ mm, $z_3 = 45.4$ mm, $x_1 = 34.2$ mm, $x_2 = 11$ mm, $x_3 = 4.29$ mm, and $x_4 = 1.79$ mm.

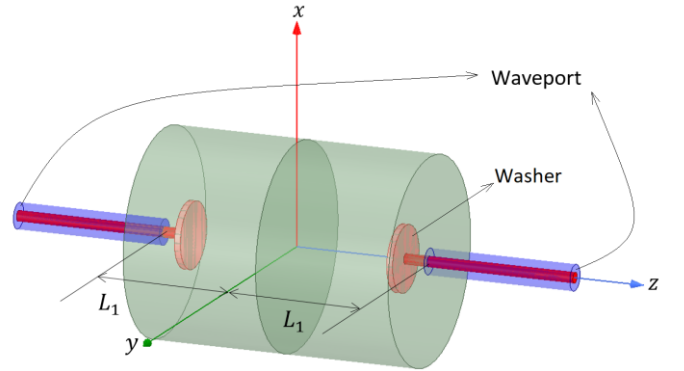


Fig. 12. Two connected CWT, $L_1 = 45.4$ mm.

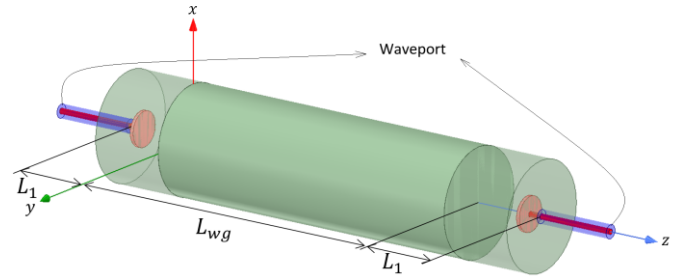


Fig. 13. Simulation of the metallic waveguide inserted between CWT, with $L_1 = 45.4$ mm and $L_{wg} = 207$ mm.

Then to be sure that the TM_{01} mode is created, a simulation with both CWT and a metallic waveguide is made according to Fig. 13.

The fields in the waveguide are plotted to verify that the TM_{01} is propagating. Fig. 14a) and 14b) validate the TM_{01} generation thanks to the CWT [45]. Indeed, the magnetic field has no components along the z -axis which is the characteristic of a TM_{mn} mode. Moreover, this field is invariant along the θ -axis, consequently, the order of the mode is 0.

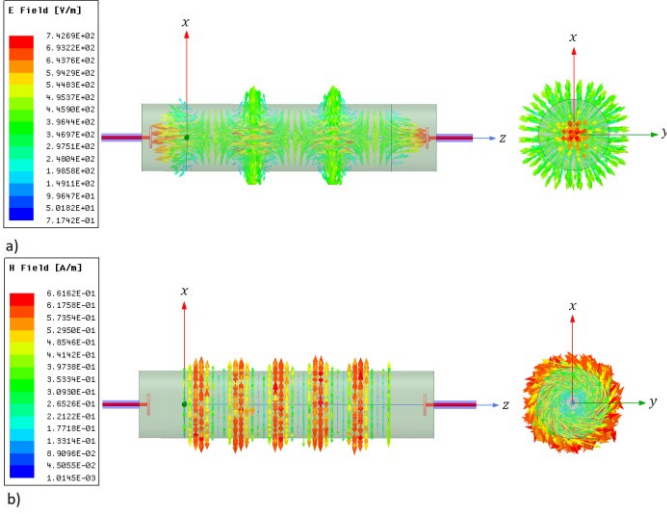


Fig. 14. a) The electric field in the metallic waveguide b) The magnetic field in the metallic waveguide.

With (3) and the Fig. 13 simulation, S-parameters of the metallic waveguide are isolated thanks to the properties of the ABCD-parameters:

$$[T_{WG}] = [T_{CWT}]^{-1}[T_{set}][T_{CWT}]^{-1}, \quad (4)$$

where $[T_{set}]$ is the chain matrix of the set displayed in Fig. 13, and $[T_{WG}]$ the chain matrix of the metallic waveguide.

With post-processing, it is possible to plot the dispersion diagrams. Indeed the k_z phase constant is related to the $\angle S_{21}$ phase of the S_{21} -parameter, by (5):

$$k_z = -\frac{\angle S_{21}}{L_{wg}}, \quad (5)$$

with $L_{wg} = 207$ mm the length of the waveguides.

2) Results

CWT are used with the corrugated waveguide according to Fig. 15. The dispersion diagram, represented in Fig. 16 with triangles, is obtained thanks to (5) and HFSS simulation of the Fig. 15a). This diagram is in agreement with the MET diagram.

The measurement setup to obtain the dispersion diagram of the corrugated waveguide is presented in Fig. 15b). The measured k_z is obtained with the same process explained in part III.B.1).

The measured dispersion diagram is represented in dashed line in Fig. 16. According to these curves, the TM_{01} is propagating in the corrugated waveguide. Moreover, the predicted k_z is in agreement with its measured values.

Thus, the TE_{11} mode is propagating in the metallic waveguide but not in the proposed corrugated waveguide. Furthermore, thanks to the new proposed CWT, the dispersion diagram of the TM_{01} has been obtained from simulations and measurements. They are very similar to the one initially expected using the MET. The TM_{01} is therefore the fundamental mode of the new proposed waveguide.

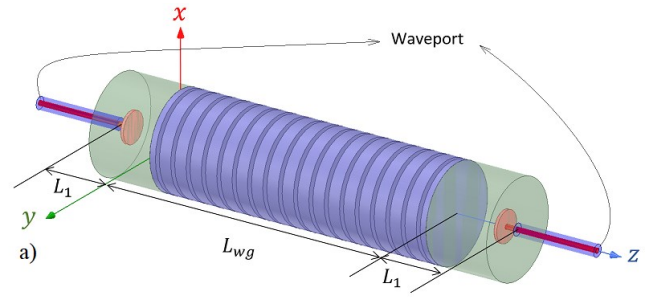


Fig. 15. a) Simulation of the corrugated waveguide in between the CWT and b) measurement setup for TM_{01} generation.

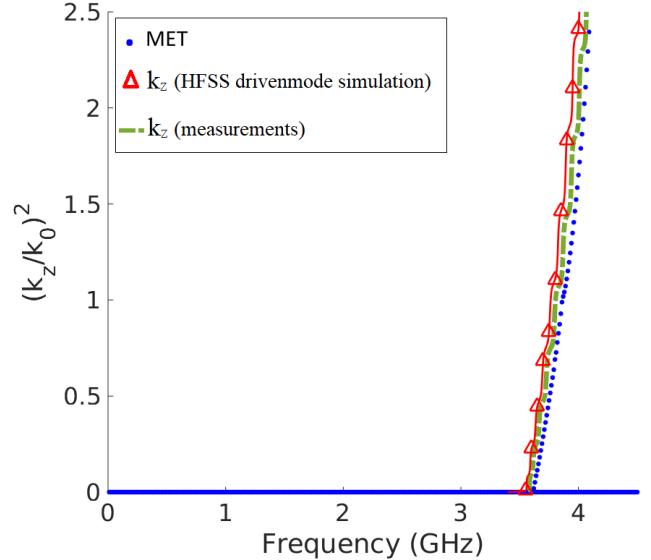


Fig. 16. Dispersion diagrams of the corrugated waveguide obtained with MET (dots), with a drivenmode HFSS simulation (triangles) and with the measurements (dashes).

IV. CONCLUSION

In this article, the MET has been used to put forward another application to metamaterial waveguides. The fundamental mode in metallic waveguide is the TE_{11} , but by adding corrugations this mode has been canceled and the TM_{01} mode became the new fundamental mode. In order to verify this, a Coaxial to Waveguide Transition has been designed to create a TM_{01} excitation. This device is used with the corrugated waveguide and with a metallic one, to verify that this mode is propagating. Moreover, the corrugated waveguide is excited with a TE_{10} rectangular waveguide similar in field distribution to TE_{11} cylindrical waveguide; as a result, no mode is propagating at all. A compact mode extractor that will separate the TE_{11} mode from the TM_{01} mode is in the fabrication phase, with the use of the corrugated waveguide

presented in this work. Some restrictions should be pointed out. Indeed, adding metamaterial wall to change the fundamental mode has some limitations: only few modes can be fundamental: the TE_{11} , the EH_{11} , the HE_{11} , the TE_{01} and the TM_{01} , as presented in the section II.A. Moreover, the MET used in this article deals only with 2-D metamaterials and $m = 0$ order mode. Nevertheless, the MET has been extended to handle all metamaterials (with or without θ invariance) and all order modes.

ACKNOWLEDGMENT

This work was made in collaboration with the CNES, MVG Industries, and the LAPLACE laboratory. The authors wish to thank O. Pigaglio for his help during the measurement campaign.

CONFLICT OF INTEREST

The authors declare no potential conflict of interest.

REFERENCES

- [1] Q. Wu, C. P. Scarborough, M. D. Gregory, D. H. Werner, R. K. Shaw, E. Lier, "Broadband Metamaterial-Enabled Hybrid-Mode Horn Antennas," in *Proc. IEEE Antennas Propag. Soc. Int. Symp. (APSURSI)*, Toronto, Canada, Jul. 2010, pp 1-4.
- [2] C. P. Scarborough, Q. Wu, M. D. Gregory, D. H. Werner, R. K. Shaw, E. Lier "Broadband Metamaterial Soft-Surface Horn Antennas," in *Proc. IEEE Antennas Propag. Soc. Int. Symp. (APSURSI)*, Toronto, ON, Canada, Jul. 2010, pp 1-4.
- [3] R. K. Shaw, E. Lier, C.-C. Hsu, "Profiled Hard Metamaterial Horns for Multibeam Reflectors," in *Proc. IEEE Antennas Propag. Soc. Int. Symp. (APSURSI)*, Toronto, Canada, Jul. 2010, pp 1-4.
- [4] E. Lier, R. K. Shaw, D. H. Werner, Q. Wu, C. P. Scarborough, M. D. Gregory, "Statuts on Meta-Horn Development - Theory and Experiments," in *Proc. IEEE Antennas Propag. Soc. Int. Symp. (APSURSI)*, Toronto, Canada, Jul. 2010, pp. 1-4.
- [5] R. A. Shelby, D. R. Smith and S. Schultz, "Experimental Verification of a Negative Index of Refraction," *Science*, vol. 292, no. 5514, pp. 77-79, Apr. 2001
- [6] D. R. Smith, W. J. Padilla, D. C. Vier, S. C. Nemat-Nasser, and S. Schultz, "Composite Medium with Simultaneously Negative Permeability and Permittivity," *Phys. Rev. Lett.*, vol. 84, no. 18, pp. 4184-4187, May 2000.
- [7] V. G. Veselago, "The Electrodynamics of Substances with Simultaneously Negative Values of ϵ and μ ," *Sov. Phys. Usp.*, vol. 10, no. 4, pp. 509-514, 1968.
- [8] R. W. Ziolkowski and E. Heyman, "Wave Propagation in Media Having Negative Permittivity and Permeability," *Phys. Rev. E, Stat. Phys. Plasmas Fluids Relat. Interdiscip. Top.*, vol. 64, no. 5, pp. 1-15, Dec. 2001, Art. no. 056625.
- [9] J. G. Pollock, A. K. Iyer, "Experimental Verification of Below-Cutoff Propagation in Miniaturized Circular Waveguides Using Anisotropic ENNZ Metamaterial Liners," *IEEE Trans. Microw. Theory Techn.*, vol. 64, no. 4, pp. 1297-1305, Apr. 2016.
- [10] J. G. Pollock, A. K. Iyer, "Below-Cutoff Propagation in Metamaterial-Lined Circular Waveguides," *IEEE Trans. Microw. Theory Techn.*, vol. 61, no. 9, pp. 3169-3178, Sep. 2013.
- [11] J. G. Pollock, A. K. Iyer, "Radiation Characteristics of Miniaturized Metamaterial-Lined Waveguide Probe Antennas," in *Proc. 2015 IEEE Int. Symp. on Antennas Propag. USNC/URSI Nat. Radio Sci. Meeting*, Vancouver, Canada, Jul. 2015, pp. 1734-1735.
- [12] J. G. Pollock, A. K. Iyer, "Miniaturized Circular-Waveguide Probe Antennas using Metamaterial Liners," *IEEE Trans. Antennas Propag.*, vol. 63, no. 1, pp. 428-433, Jan. 2015.
- [13] B. Byrne, N. Raveu, N. Capet, G. Le Fur, L. Duchesne, "Reduction of Rectangular Waveguide Cross-Section with Metamaterials: A New Approach," in *Proc. 9th Int. Congr. on Adv. Electrom. Mat. Microw. Opt. (METAMATERIALS)*, Oxford, U.K, Sep. 2015, pp. 40-42.
- [14] B. Byrne, Etude et Conception de Guides d'Onde et d'Antennes Cornets à Métamatériaux, Ph. D. dissertation, Thèse de Doctorat de l'université de Toulouse, 8 Novembre 2016.
- [15] P.-S. Kildal, E. Lier, "Hard Horns Improve Cluster Feeds of Satellite Antennas," *Electron. Lett.*, vol. 24, no. 8, pp. 491-492, Apr. 1988.
- [16] H. C. Minnett, B. MacA. Thomas, "A Method of Synthesizing Radiation Patterns with Axial Symmetry," *IEEE Trans. Antennas Propag.*, vol. 14, no. 5, pp. 654-656, Sep. 1966.
- [17] E. Lier, "Review of Soft and Hard Horn Antennas, Including Metamaterial-Based Hybrid-Mode Horns," *IEEE Trans. Antennas Propag. Mag.*, vol. 52, no. 2, pp. 31-39, Apr. 2010.
- [18] B. Byrne, N. Capet, N. Raveu, "Dispersion Properties of Corrugated Waveguides Based on the Modal Theory," in *Proc. EUCAP 2014: 8th European Conf. Antennas Propag.*, The Hague, Netherland, 2014.
- [19] N. Raveu, B. Byrne, L. Claudepierre and N. Capet, "Modal Theory for Waveguides with Anisotropic Surface Impedance Boundaries," *IEEE Trans. Microw. Theory Techn.*, vol. 64, no. 4 pp. 1153-1162, Apr. 2016.
- [20] B. Byrne, N. Raveu, N. Capet, G. Le Fur and L. Duchesne, "Modal analysis of Rectangular Waveguides with 2D Metamaterials," *Prog. Electromagn. Res. C*, vol. 70, pp. 165-173, 2016, doi: 10.2528/PIERC16092904.
- [21] L. Kuhler, G. Le Fur, L. Duchesne, N. Raveu, "The Propagation Characteristics of 2-D Metamaterial Waveguides Using the Modal Expansion Theory," *IEEE Trans. Microw. Theory Techn.*, vol. 66, no. 10, pp. 4319-4326, Oct. 2018.
- [22] L. Kuhler, G. Le Fur, L. Duchesne, N. Raveu, "Modal Analysis of Cylindrical Waveguides with 2-D Metamaterial Wall," in *Proc. META 2018 - The 9th Int. Conf. Metamaterials, Photonic Crystals Plasmonics*, Marseille, France, 2018.
- [23] L. Kuhler, N. Raveu, G. Le Fur, L. Duchesne, "Théorie Modale Élargie Appliquée aux Guides d'Onde Cylindriques à Métamatériaux," in *Proc. XXIème Journées Nationales Microondes*, Caen, France, 2019.
- [24] P. K. Verma, R. Kumar, M. Singh, "Design of a Shaped Omni-Directional Circular Waveguide Antenna," in *Applied Electromagn. Conf. (AEMC)*, Kolkata, India, Dec. 14-16 2009.
- [25] J. Tang, L. Fang, H. Cheng, "A Low Sidelobe and High Gain Omni-Directional COCO Antenna Array," in *Proc. Asia-Pacific Conf. Antennas Propag. (APCAP)*, Harbin, China, Jul. 26-29 2014.
- [26] I. Güngör, A. Ünal, "Design of a Vertically Polarized Omni-Directional Antenna at Ka-Band," in *IEEE Int. Symp. Antennas Propag. (APSURSI)*, Fajardo, Puerto Rico, 26 Jun.-1 Jul. 2016.
- [27] S. Champeaux, P. Gouard, R. Cousin, J. Larour, "3-D PIC Numerical Investigations of a Novel Concept of Multistage Axial Vircator for Enhanced Microwave Generation," *IEEE Trans. Plasma Science*, vol. 43, no. 11, pp. 3841-3855, Nov. 2015.
- [28] S. Champeaux, P. Gouard, R. Cousin, J. Larour, "Improved Design of a Multistage Axial Vircator With Reflectors for Enhanced Performances," *IEEE Trans. Plasma Science*, vol. 44, no. 1, pp. 31-38, Jan. 2016.
- [29] R. Baldwin, P. A. McInnes, "Corrugated Rectangular Horns for Use as Microwave Feeds," *Proc. Inst. Electr. Eng.*, vol. 122, no. 5, pp. 465-469, May 1975.
- [30] A. Bromborsky, B. Ruth, "Calculation of the TM_{0n} Dispersion Relations in a Corrugated Cylindrical Waveguide," *IEEE Trans. Microw. Theory Techn.*, vol. 32, no. 6, pp. 600-605, Jun. 1984.
- [31] P. J. B. Clarricoats, "Analysis of Spherical Hybrid Modes in a Corrugated Conical Horn," *Electronics Lett.*, vol. 5, no. 9, pp. 189-190, May 1969.
- [32] P. J. B. Clarricoats, A. D. Olver, S. L. Chong, "Attenuation in Corrugated Circular Waveguides. Part 1: Theory," *Proc. Inst. Electr. Eng.*, vol. 122, no. 11, pp. 1173-1179, Nov. 1975.
- [33] J. Esteban, J. M. Rebolgar, "Characterization of Corrugated Waveguides by Modal Analysis," *IEEE Trans. Microw. Theory Techn.*, vol. 39, no. 6, pp. 937-943, Jun. 1991.

- [34] G. L. James, "Analysis and Design of TE₁₁-to-HE₁₁ Corrugated Cylindrical Waveguide Mode Converters," *IEEE Trans. Microw. Theory Techn.*, vol. 29, no. 10, pp. 1059-1066, Oct. 1981.
- [35] H. S. Lee, "Dispersion Relation of Corrugated Circular Waveguides," *J. Electromagn. Waves Appl.*, vol. 29, no. 10, pp. 1391-1406, Jan. 2005.
- [36] B. MacA. Thomas, H. C. Minnett, "Modes of Propagation in Cylindrical Waveguides with Anisotropic Walls," in *Proc. Institution of Electrical Eng.*, vol. 125, no. 10, pp. 929-932, Oct. 1978.
- [37] D. M. Pozar, "Microwave Engineering," John Wiley & Sons, ISBN 0-471-17096-8, 1998.
- [38] S. B. Chakrabarty, V. K. Singh, S. Sharma, "TM₀₁ Mode Transducer Using Circular and Rectangular Waveguides," *Int. J. RF Microw. Computer-Aided Eng.*, vol. 20, no. 3, pp. 259-263, May 2010.
- [39] A. Chittora, S. Singh, A. Shama, J. Mukherjee, "Design of Wideband Coaxial-TEM to Circular Waveguide TM₀₁ Mode Transducer," in *Proc. 10th European Conf. Antennas Propag. (EuCAP)*, Davos, Switzerland, 10-15 Apr. 2016.
- [40] L. Guo, W. Huang, H. Shao, Y. Liu, J. Li, T. Ba, Y. Jiang, "A Novel Two-Way TM₀₁ Mode Combiner for High Power Microwave Applications," *Prog. Electromagn. Res. Symp. (PIERS)*, Shanghai, China, 8-11 Aug. 2016.
- [41] X.-M. Li, J.-Q. Zhang, X.-Q. Li, Q.-X. Liu "A High-Power Orthogonal Over-Mode Circular Waveguide TE₁₁-TM₀₁ Mode Converter," *IEEE Microw. Wireless Components Lett.*, vol. 27, no. 12, pp. 1095-1097, Dec. 2017.
- [42] J. R. Montejó-Garai, J. A. Ruiz-Cruz, J. M. Rebollar, "Design of a Ku-Band High-Purity Transducer for the TM₀₁ Circular Waveguide Mode by Means of T-Type Junctions," *IEEE Access*, vol. 7, pp. 450-456, Dec. 2018.
- [43] A. Tribak, J. Zbitou, A. Mediavilla Sanchez, N. Amar Touhami, "Ultra-Broadband High Efficiency Mode Converter," *Prog. Electromagn. Res. C*, vol. 36, pp. 145-158, 2013.
- [44] D. A. Frickey, "Conversions Between S, Z, Y, H, ABCD, and T Parameters Which are Valid for Complex Source and Load Impedances," *IEEE Trans. Microw. Theory Techn.*, vol. 42, no. 2, pp. 205-211, Feb. 1994.
- [45] C. S. Lee, S. W. Lee, S. L. Chuang, "Plot of Modal Field Distribution in Rectangular and Circular Waveguides," *IEEE Trans. Microw. Theory Techn.*, vol. 33, no. 3, pp. 271-274, Mar. 1985.



Lucille Kuhler was born in Metz, France, in 1992. She received the M.Sc. degree in aeronautical and space telecommunications engineering from the ENAC (French Civil Aviation University), Toulouse, France, in 2016 and the Ph. D. degree in electromagnetism and microwaves from the INPT (National Polytechnic Institute), Toulouse, in 2019.

Her Ph.D. thesis was on cylindrical waveguides with metamaterial. In 2019, she joined the TELECOM/EMA research axis at the ENAC as a research engineer. She is currently working on propagation models and EMC solutions for CNS systems, on behalf of the French Civil Aviation Directorate.



Nathalie Raveu received the M.S. degree in electronics and signal processing in 2000 and the Ph. D. degree in 2003.

She is a Professor with the National Polytechnic Institute of Toulouse (INPT) and a Research Fellow with the LAPLACE - CNRS (Laboratory of PLasma and Energy Conversion).

Her research topics are oriented toward development of efficient numerical techniques to address innovative microwave circuits. During the last years, she has developed a new method for SICs study, metamaterial horns, and plasma cavity.



Gwenn Le Fur received the M.S. degree in signal processing and telecommunications from the University of Rennes 1, Rennes, France, in 2006 and the Ph.D. degree from the Rennes Institute of Electronics and Telecommunications, Rennes, France, in 2009.

He was first with the CEA LETI, Grenoble, France, where he worked on characterization of small antenna using noninvasive measurement methods and integrated multi-antenna system. Then he joined SATIMO industries (Microwave Vision Group) as a R&D Engineer. He is now with the Centre National d'Etudes Spatiales (CNES), Toulouse, France, working on antenna measurement techniques.



Luc Duchesne got his diploma of engineer in electronics in 1992 from Ecole Supérieure d'Electronique de l'Ouest (ESEO), Angers, France and then a specialization in aerospace electronics in 1994 from Ecole Nationale Supérieure de l'Aéronautique et de l'Espace (ISAE - Supaéro), Toulouse, France.

He started his professional life in 1994 at Deutsche Aerospace (Dasa) in Munich (now Airbus Defence and Space) as an Antennas and Payload Components Engineer.

In August 2000, he joined SATIMO close to Paris (Now Microwave Vision) as Research and Development Director. From 2000 on to present, he participated to build a strong R&D department within SATIMO dedicated to the development of innovative products for the core activity of antenna measurement systems but also for new activities concerning non-destructive testing systems and imagery systems.

He co-authored several conference papers about antennas and antenna measurement systems. He is also co-inventor of several patents at DASA and SATIMO.